Chapter 2
Basic Information for Design of Particulate Products

Henk G. Merkus

Good correlation between parameters is fine,
Some added understanding is better.

Abstract In this chapter some basic features of particulate products are examined, which are relevant for adequate design and best performance. Particle packing and product porosity is considered first. Closest packing is reached within size distributions, where small particles fill the voids in between the larger particles. Smallest void fractions in monosized powders are reported to be about 40 % (related solids content 60 %); the ideal void fraction is 26 %. For polydisperse powders, especially those containing polymodal size distributions minimum void fractions may be considerably smaller and maximum packing densities larger. Powder flow and cohesivity strongly depend upon particle size and shape. Various empirical values for the characterization of flowability are presented. In general, it can be said that dry powders having a particle size above 50 μm and regular particle shape, flow easily. When the particles are much smaller and/or when they have a large aspect ratio, they tend not to flow at all: they are called cohesive. The fluidization of powders follows a similar trend where granular particles in the 20–200 μm size range fluidize readily and smaller particles together with ones of high aspect ratio, can cause difficulties. Geldart has categorized powders as cohesive, aeratable, bubbling and spouting; the latter two words mean that particles larger than about 200 μm show another 'fluidization' behavior. Equations for fluid flow through packed beds are developed by different authors. The equation of Carman and Kozeny is used in filtration. The viscous behavior of emulsions and suspensions is strongly related to particulate concentration. At low concentrations, the viscosity shows a Newtonian behavior; it is independent of particle size and

H.G. Merkus (✉)
Retired Associate Professor, Delft University of Technology, Park Berkenoord 30, Pijnacker 2641 CZ, The Netherlands
e-mail: henkmerkus@hetnet.nl

H.G. Merkus and G.M.H. Meesters (eds.), *Particulate Products: Tailoring Properties for Optimal Performance*, Particle Technology Series 19,
DOI 10.1007/978-3-319-00714-4_2,

relates linearly with concentration. At high concentrations, various types of non-Newtonian behavior exist. Viscosity depends on particle size (distribution), but is no longer linearly related to particulate concentration. Differences between solids concentration and maximum packing density of the particles play an important role. Moreover, rheological behavior may be time-dependent through changing particle-particle or molecular interactions. Adequate non-Newtonian behavior is essential for good performance during production and for the final quality of various products, such as chocolate, ice cream and paint dispersions. Long-term stability of dispersions often relates to the zeta-potential. Absolute values of at least about 50 mV can cause stable dispersions. At low zeta-potential values, the particles tend to agglomerate or flocculate. Dispersion stability may be improved by application of steric stabilizers. In paint, color, scattering, transparency and hiding power of dispersed particles are also strongly related to particle size and shape. Several equations are provided that are useful in the design of pigment mixtures. These aspects play a role in human appreciation of paints, foods and creams. Sensorial characteristics are important in foods, sweets, beverages and cosmetics. Some terminology is provided. Interpretation of some of the terminology is subjective. This is due to the characteristics not only having a physical background but may also relate to particle size and shape, psychological or cultural aspects. Finally, this chapter deals with the adsorption and diffusion of components into the pores of adsorbents and catalysts. In such cases the diffusion rate is strongly linked to the pore size distribution and the effective molecular size of the diffusing component.

2.1 Introduction

Particle characteristics play an important role in the quality aspects of particulate products. In general, they have an effect on e.g. particle packing, sensorial aspects, transparency and hiding power as well as on adsorption, catalysis and separations. In the case of dry powders, there is a relationship with powder flow and fluidization. For emulsions and suspensions, they affect rheological properties in a positive or negative way. These effects and existing relationships will be treated in the following paragraphs.

2.2 Particle Packing and Product Porosity

Particle packing is of fundamental importance for powders. It has influence with respect to the mass of powder in a given volume and thus the dose of drug in a tablet. It also influences their flow properties, which in turn affects powder operations like the flow from hoppers. Moreover, a higher degree of packing causes less shrinkage during sintering and better product strength in ceramics and concrete. Particle packing is usually expressed as (effective) powder density, product

porosity or void fraction. A higher degree of packing means a higher powder density and less voids between the particles, and vice versa. The void fraction ε is defined by:

$$\varepsilon = \frac{V_V}{V_B} = 1 - \frac{V_P}{V_B} = 1 - \frac{\rho_B}{\rho_e} = 1 - \frac{M}{\rho_e V_B} \tag{2.1}$$

where:

ε = void fraction in powder bed (powder bed porosity)
V_V = volume of voids
V_B = volume of powder bed
V_P = volume of particles in bed
ρ_B = effective bulk density of powder bed
ρ_e = envelope particle density (including all intra-particle pores)
M = mass of powder bed

The degree of particle packing is related to the number and area of contacts between particles and is governed by the attractive and the frictional forces between the particles. The way that a packing is prepared has an important influence on the degree of packing. For example, tapping (vibration) usually enables particles in a loose powder to take positions in closer proximity. Tapped powder density can be considerably larger than the density in loose packing. Particle size, size distribution and particle shape may have a substantial influence (see below).

The closest packing of monosized spheres contains about 26 % voids, regardless of particle size [8, 51]. Thus, about 74 % of the overall volume is taken by the particles. This maximum is reached in a regular, rhombohedral particle arrangement, where each sphere touches 12 neighbors. It can only be reached by careful building of the particle arrangement, but never in general powders. In the case of large, monosized, smooth spheres, friction between particles causes the packing density to be considerably lower than the above maximum, and thus powder porosity is larger. Maximum density for random packing, obtained by careful vibration, appears to be 63.7 % v/v [69]. Less careful mixing, imperfect spheres and surface roughness increasing packing resistance, results in still lower packing densities with void fractions larger than 40 % v/v [8, 77]. The influence of particle size becomes important for sizes below about 20 μm. Decreasing particle size leads to stronger attractive forces (mainly Van der Waals- type for dry powders) between particles, also causing more difficult particle rearrangements. Typical porosity of dry particle beds increases for particles smaller than about 20 μm. Note that presence of moisture strongly increases adhesive forces between particles.

In the case of free-flowing powders (size distribution width, D_{90}/D_{10} 1.5–10 and particle size D_{90} above about 20 μm), the inter-particle voids may be filled, in principle, with smaller particles. In practice, a minimum void fraction of about 25 % v/v can be attained under these conditions (75 % v/v solids) [8, 51, 77]. Optimum polymodal mixtures may result in still higher densities for random packing, up to about 85 % v/v. Size ratios as well as relative quantities of the modes should

be attuned in such a way that the finer particles exactly fill the voids left by the larger particles [19, 55].

If a high degree of packing, approaching the maximum, is desirable as in ceramics or concrete, it may be reached through the addition of a liquid to form a paste, which reduces the inter-particle friction.

Small amounts of specific solid ingredients may give the same result as well as reducing the liquid content (see e.g. Sect. 2.3 and Chap. 7).

As stated above, the density of particle packing in powders decreases progressively with increasing ratio of attractive forces between particles and inter-particle friction to the gravity force for particles. The attractive forces and inter-particle friction depend upon surface area (size squared) and particle shape. The gravitational force depends upon mass (size cubed). Therefore, powder cohesivity increases with decreasing particle size and increasing surface roughness. An empirical relationship between powder porosity and particle size, has been reported for the gravitational packing (both poured and tapped) for irregularly shaped fused alumina powders, having a particle size greater than 1 μm [87].

$$\varepsilon = \varepsilon_0 + (1 - \varepsilon_0)\exp\left(-aD_{50;3}^{b}\right) \tag{2.2}$$

where:

ε = powder bed porosity (void fraction in powder bed)
ε_0 = limiting porosity (in either tap density or some effective bed density)
$D_{50;3}$ = median particle size of volume-based size distribution
a = powder packing factor (depends on way of packing)
b = particle shape factor

For cohesive powders, where attractive forces between the particles are large, the degree and ease of packing depends on the size and strength of existing agglomerates. This size can be expressed in an equivalent packing size [87]. A power-law relation was determined between the ratio of equivalent packing size[1] $r_{i,j}$ between components i and j and the corresponding equivalent volume diameter $R_{i,j}$ for bimodal mixtures:

$$r_{i,j} = R_{i,j}^{p} \tag{2.3}$$

where:

p = powder packing exponent (this depends on way of packing and strength of attractive forces)

Note that the constants in the above equations depend on the interactive forces between the particles and, thus, depend on the product composition.

[1] The equivalent packing size represents the size of agglomerates, which act as (composed) particles during packing.

The effect of particle shape on the degree of packing becomes significant when the particles have a flat or rough surface or a large aspect ratio, such as with plates and fibers. Such particles tend to be more cohesive than spheres or irregular particles. One reason is the increased surface for inter-particle contacts, which leads to increased attractive forces. A rough particle surface causes larger friction between particles. Fibers have a larger difficulty for free movement due to their length being prone to causing entanglement. Extreme examples are fibers of glass or asbestos. Thin-cut potato crisps with their curved platelet structure, provides a nice example of the influence of particle shape. The irregular structure of the conventional type causes an extremely loose packing. The structure of a newer type (Kellogg's Pringles) where all crisps have the same shape, on the other hand, allows a very close (platelet-like) packing, but only after careful construction of the packing. Flat mica platelets are capable of extremely close packing as realized by nature.

2.3 Powder Flow and Fluidization

Flowability, cohesivity and fluidization are important characteristics of dry particulate materials. Critical examples are emptying of hoppers, mixing or dosing of powders, or use of particulate materials in catalytic processes. A particle size of at least about 20–50 μm and regular particle shape are required for good flow behavior. Note that the presence of moisture in powders may also cause poor flow properties through hydrogen bonding or capillary forces [17].

A. **Powder Flow**

Dry powders show large differences in flow behavior. Some flow very easily; others flow not at all: they are called cohesive. The differences depend upon particle size, shape and surface roughness. Although there has been considerable progress in understanding bulk powder behavior, much work needs to be done to develop the functional relationships between particles and bulk powders with respect to flowability [5, 20, 51, 54].

Differences in flowability/cohesivity of dry powders can easily be seen by comparing powdered sugar used for icing cakes (particle size about 1 μm) and crystal sugar (particle size about 400 μm). The former behaves as a cohesive powder; the latter is free-flowing, which makes flow and dosing much easier. The same holds for detergents (dry powder versus compacted pearls). In the general case of dry powders, the differences are caused by Van der Waals forces, which are related to the surface-to-volume ratio of the particles. For hygroscopic powders, such as detergents, flow properties are often deteriorated by the presence of moisture, due to their hygroscopic nature.

The surface-to-volume ratio increases with decreasing particle size, which in turn causes an increased inter-particle attraction. If the powder has undergone some compaction, by its own weight and/or by vibration or tapping, then the number of contacts between the particles increases. This can not only lead to stronger cohesivity but at its limit significantly increases the mechanical strength of the

compressed powder. For particles smaller than about 20 μm and having an aspect ratio of about 1, the attractive forces cause agglomeration of the particles. This means that such powders are cohesive and do not flow easily. If de-agglomeration of such particles is needed, strong shear forces are required, until the point where particle bonding in the clumps is too strong. Sometimes, a small amount of sub-micrometre particles (e.g. fumed silica) can be added to improve flowability. For particles larger than about 50 μm and having an aspect ratio of about 1, the attractive forces are insignificant and the resistance to flow is only caused by friction. Then, these powders are free-flowing. Segregation in a batch of particles, according to size may be expected. Increased aspect ratios, such as in the case of fibers and plates, also causes decreased flowability, as the number of contact points between particles is increased.

In practice, the Carr Compressibility Index *CI* or the related Hausner Ratio *H* are often used to indicate the both compressibility and flowability [9, 81]:

$$CI = 100\frac{V_f - V_t}{V_f} = 100 \times \left(1 - \frac{\rho_f}{\rho_t}\right) = 100 \times (1 - 1/H) \tag{2.4}$$

and:

$$H = \frac{V_f}{V_t} = \frac{\rho_t}{\rho_f} \tag{2.5}$$

where:

CI = Carr Compressibility Index (%)
H = Hausner Ratio
V_f = freely settled volume per unit mass of powder
V_t = tapped volume per unit mass of powder
ρ_f = freely settled bulk density of powder
ρ_t = tapped bulk density of powder

A simple, popular test for flowability is the measurement of the angle of repose of a cone-like heap of powder after dropping it onto a fixed base plate from a funnel at some elevation. The angle of spatula, the Jenike and similar shear tests, the flow rate through an orifice (the latter only for free flowing materials) and avalanching tests are also used [21, 36, 37, 45, 46, 53, 82]. For the mass flow from a hopper, the wall friction and the corresponding critical angle also influences the flowability [52]. Some values for classification of the flow properties of powders are given in Table 2.1.

Table 2.1 Classification of flow properties of powders

Flow property	Carr index (%)	Hausner ratio	Angle of repose, degrees
Excellent	≤ 10	1.00–1.11	25–30
Good	11–15	1.12–1.18	31–35
Fair; aid not needed	16–20	1.19–1.25	36–40
Passable; borderline	21–25	1.26–1.34	41–45
Poor; must agitate, vibrate	26–31	1.35–1.45	46–55
Very poor	32–37	1.46–1.59	56–65
Very, very poor	≥ 38	≥ 1.60	> 66

For example, Carr Index < 15, Hausner Ratio < 1.18 and Angle of Repose $< 35°$ are considered as indications for good flowability, compared with Carr Index > 25, Hausner Ratio > 1.34 and Angle of Repose $> 45°$ for poor flowability.

Compression (consolidation) of a powder, which already may occur during storage under its own weight, will decrease flowability, as the number of point contacts and Van der Waals forces increase. The effect of consolidation can be tested in shear cells.

Note that small amounts of moisture increases cohesivity of powders significantly [53]. Typically, flowability gets worse with increasing moisture content due to formation of liquid bridges between particles. At a certain moisture content, maximum cohesivity is reached. At still higher moisture contents, the liquid starts acting as a glidant and flowability increases. When all voids are filled, the powder reaches the state of a paste or a slurry.

Taylor et al. [81] have applied principal component analysis to reveal a flowability index for pharmaceutical powders based on measurements of critical orifice, compressibility and angle of repose. They conclude that a combined index provides a better characterization of powder flow than the individual tests. This is due to the fact that the different tests challenge different aspects of the complex flow behavior of powders.

Extensive research has not yet lead to an adequate understanding and basic relationships between the flowability of powders and the size and shape characteristics of the constituting particles.

B. **Fluidization**

When a fluid is passed upwards through a packed bed of particles that is unrestrained at its upper surface, there is an increase of the frictional resistance and pressure loss in the fluid with increasing flow rate. At some point, the upward drag force of the fluid on the particles becomes equal to the mass of the particles in the bed and the pressure drop remains constant with increasing flow. Often some excess pressure is required to free the particles from adhesion or interlocking. Four groups of powders can be distinguished, as shown in the classical Geldart diagram. The distinction has been found empirically for powders when exposed to dry air at ambient pressure and temperature (Fig. 2.1) [20, 84].

Type C powders, with particle size smaller than about 20–80 μm (depending on density difference ρ_P-ρ_F of particles and fluid) are cohesive. Such powders cannot be fluidized by a stream of fluid. When subjected to a gas flow, the gas passes in channels through the powder or lifts slugs of particles. For these powders, the attractive forces between particles are much greater than particle mass [84].

Type A powders with larger particles, sizing from tens to hundreds micrometers, are aeratable. They can be fluidized in an upward gas flow above minimum fluidization velocities. In these powders, the attractive forces between the particles are in the same order of magnitude as their mass. Upon aeration of the powder, the powder bed expands considerably without bubbles being formed. A fluidized bed behaves like a liquid, in which the particles are subject to weak attractive forces [21]. This type of

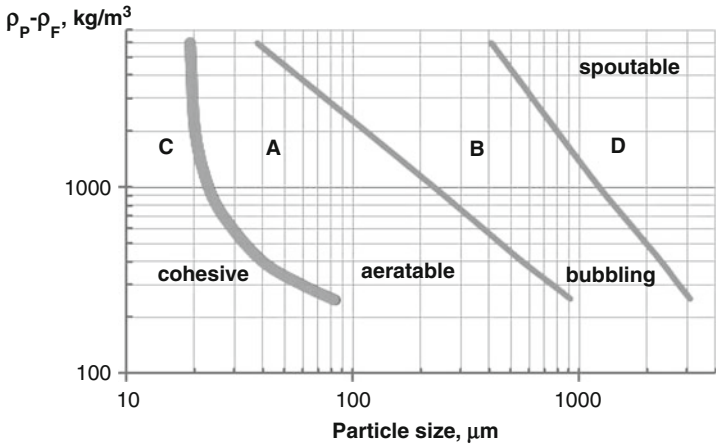

Fig. 2.1 Geldart fluidization diagram (Adapted from [20])

behavior is important e.g. in catalytic reactions where it provides optimum contact between gaseous reactants and solid catalyst particles, in addition to adequate temperature control.

Type B powders, again larger particles start forming bubbles as soon as the lifting force of the fluid velocity exceeds the particle mass. Particle mass is much greater here than inter-particle forces. The bubbles coalesce as they rise through the bed. When they take up the size of the cross section of the bed, they may cause 'slugging', i.e. lift a section of the bed contents over a short distance until the particles drop down again.

Type D powders contain still larger particles. Bubbles are also formed here but the required fluid velocity is so high and the particles so heavy, that these 'bubbles' bypass the solids in so-called spouts. These spouts are fluid jets, which entrain some particles upwards and let them fall back again later at the sides of the jets.

In all cases, particles are blown out of the bed at very high fluid velocities, when the lifting forces are larger than particle mass.

For the fluidization regime, it can be derived that [21, 64, 70]:

$$\frac{\Delta P}{H_b} = \left(1 - \varepsilon_{fl}\right)\left(\rho_P - \rho_F\right)g \tag{2.6}$$

where:

ΔP = pressure drop over bed
H_b = bed height
ε_{fl} = void fraction during fluidization
ρ_P = effective density of particles
ρ_F = density of fluid
g = gravitational acceleration constant

Several empirical relationships have been derived for the minimum fluidization gas velocity in relation to particle size [64].

The understanding of fluidization behavior has significantly increased in the last decades and methods for improvement for cohesive powders have been published [84]. For example, some powders can sometimes be fluidized through weakening of the attractive inter-particle forces, i.e. by addition of a small amount of nano-particles that adhere to the particulate surface, or through modification of temperature, fluid viscosity or pressure. Additionally, mechanical vibration or application of an external electric or magnetic field have been applied. It has also been found that some nano-particles aggregate/agglomerate to form clusters having sizes of tens of micrometers and low density, which can be fluidized.

2.4 Fluid Flow Through Particulate Beds

Darcy has found that the volumetric flow rate of a liquid in a channel is proportional to the pressure drop and inversely proportional to the liquid viscosity under laminar flow conditions [1, 8, 22, 64]:

$$\Phi_v = \frac{\Delta P}{\eta_L \cdot K} \tag{2.7}$$

where:

Φ_v = volumetric flow rate
ΔP = applied pressure drop
η_L = liquid viscosity
K = resistance constant depending on channel geometry

Later, Hagen and Poiseuille derived (independently) a similar but more specific equation for laminar flow of fluids through circular capillaries:

$$< u >= \frac{d^2}{32\eta_F} \frac{\Delta P}{L} \tag{2.8}$$

where:

$< u >$ = mean linear fluid velocity
d = diameter of capillary
η_F = fluid viscosity
L = length of capillary

The volumetric flow rate Φ_v can be derived from $< u >$ since:

$$\Phi_v = \frac{\pi \cdot d^2 \cdot < u >}{4} \tag{2.9}$$

Later again, Carman and Kozeny worked out an equation for laminar fluid flow through a non-compressible, randomly packed fixed bed of solid, monosized, spherical particles by considering the bed pores equivalent to a set of parallel capillaries. They assumed the particle surface of the bed, which relates to the particle diameter squared, per unit volume of pore space to be the important factor for bed permeability:

$$< u_s >= \frac{D^2 \cdot \varepsilon^3}{180\eta_F(1-\varepsilon)^2} \frac{\Delta P}{H_b} \tag{2.10}$$

where:

$< u_s >$ = mean linear superficial fluid velocity
D = spherical particle diameter
ε = bed porosity (void fraction)
H_b = bed height

Note that the constant factor 180 is an approximation and includes factors relating to particle shape and channel tortuosity. The value of this 'constant' may depend somewhat on particle size range and bed porosity.

In the case of non-spherical particles in a particle size distribution, particle diameter D should be replaced by the surface weighted (or Sauter) mean diameter $D_{3,2}$ in Eq. 2.10. The Kozeny-Carman equation is most often used for estimating conditions in industrial filtration.

In the above equations, viscosity only depends on the type of fluid and the temperature.

2.5 Rheology of Emulsions and Suspensions

The rheology of industrial emulsions and suspensions is of particular interest in relation to processability, stability and applicability of such products. Moreover, some sensorial aspects relate to rheological behavior (see Sect. 2.8).

The Newtonian flow model, which is used to describe the flow of a gas, a liquid or a dilute dispersion, is the most well-known. The Eqs. 2.7, 2.8, and 2.10 are special cases of the Newtonian flow. In this model, the required force (shear stress) to maintain flow is proportional to the shear (strain[2]) rate, with the viscosity as the proportionality constant. In other words, the viscosity is a measure of the resistance of a fluid to flow [22, 25, 28, 49, 51, 80]:

[2] For solids, strain can be seen as deformation.

$$\tau = \eta_L \left(\frac{d\gamma}{dt} \right) \tag{2.11}$$

where:

τ = shear stress (force per unit area)
η_L = liquid (Newtonian) viscosity
$(d\gamma/dt)$ = shear rate (or shear strain rate)

The rheological behavior of particulate dispersions depends on the particulate concentration and – at high particulate concentrations – also on the particle size, size distribution (PSD) and particle shape.

(A). **Particulate concentration**

The viscosity of dilute dispersions of spherical particles increases with the concentration of particles [14, 22, 28, 48, 49, 51, 55, 65, 71, 72]:

$$\eta_d = \eta_L (1 + 2.5\Phi) \tag{2.12}$$

or:

$$\eta_{rel} = \eta_d / \eta_L = 1 + 2.5\Phi \tag{2.13}$$

where:

η_d = viscosity of dispersion
η_L = viscosity of pure liquid
η_{rel} = relative viscosity of dispersion
Φ = effective volume fraction of dispersed phase (involving the hydrodynamic diameter)

The constant factor 2.5 in the equations is named the Einstein constant [15]. Other names for this constant are intrinsic viscosity or limiting viscosity number of particles, i.e. their contribution to the viscosity of a dispersion. This linear relationship only holds for dilute dispersions of rigid spheres, which have the same size and no interaction. In such cases, inter-particle distance must be large and concentration low (less than about 5 % v/v). Moreover, the proportionality constant of 2.5 in Eqs. 2.12 and 2.13 may have to be adapted somewhat in relation to particle shape, for shapes that deviate significantly from spherical. No dependency on particle size has been found in the absence of particle-particle interaction.

Electrical interactive forces between particles may lead to an increased viscosity in comparison to Eqs. 2.12 and 2.13, through the electro-viscous effect. In such cases the intrinsic viscosity (above: 2.5) may have to be doubled, even at concentrations below 5 % [28].

In most dispersions having an intermediate concentration range (up till about 30 % v/v), particulate concentration oversteps the limits for a linear relationship as particle-particle interactions may occur. For the case of rigid, non-interacting

spheres, an extended form of the Einstein equation has been derived, known as the Brinkmann-Roscoe equation [6, 16, 66]:

$$\eta_{rel} = (1 - \Phi)^{-2.5} \tag{2.14}$$

Note that, for small particulate concentrations, Eq. 2.14 is similar to Eq. 2.13.

More complex equations have been proposed, but all appear to lack general validity [63, 71, 72]. In the absence of a general theory, the relation between the relative viscosity and particulate concentration is often approximated by a polynomial [13, 28, 48, 71, 72, 76]:

$$\eta_{rel} = 1 + c_1 \cdot \Phi + c_2 \cdot \Phi^2 + c_3 \cdot \Phi^3 + ... \tag{2.15}$$

Here, c_1, c_2, c_3 are proportionality constants of an estimated polynomial, in which the squared term may be assumed to account for binary particle interactions, the cubed term for ternary interactions, etc.

In general, the viscosity not only depends on particle size and particle size distribution but also upon the type of fluid, electrolyte, surfactant, zeta-potential of particles, particulate concentration, temperature and interactive forces (Van der Waals or electrostatic). The relationship with particle size is an inverse one: smaller particles cause higher viscosity at the same concentration, due to higher number per unit volume and larger surface area. This dependency is expressed in the constants c_1, c_2, etc., which strongly depend upon the components in the product and the conditions of the application.

For colloid dispersions close to maximum packing (see Sect. 2.2), several equations relate the viscosity to the relative fraction of particulates in comparison to the maximum packing. This fraction also depends upon the size distribution, as indicated earlier. One example is provided by the Krieger-Dougherty equation [41]:

$$\eta_{rel} = \left(1 - \frac{\Phi_e}{\Phi_m}\right)^{-c\Phi_m} \tag{2.16}$$

where:

Φ_e = effective particulate fraction
Φ_m = particulate fraction of maximum packing
c = constant (intrinsic viscosity; often close to the Einstein value of 2.5)

Note that the effective fraction of particulates in dispersions is often increased by adsorbed molecules (dispersant and liquid) and by electric and/or steric repulsion between particles.

The general case of concentrated industrial mixtures is even more complex, as they often show non-Newtonian behavior, i.e. the dependency of viscosity on shear rate and exposure time. Here too, the difference between actual particulate concentration and the concentration in densest packing determines the rheological

behavior. In fact, electric and steric effects, relevant to particle-particle interactions, as well as additives are often used deliberately to cause some kind of network 'structure' in the product. In these circumstances a sensitivity exponent has to be added to the shear rate ($d\gamma/dt$). This is often indicated as [22, 23, 39, 50, 51, 55]:

$$\eta_m = \eta_0 \left(\frac{d\gamma}{dt}\right)^{m-1} \tag{2.17}$$

where:

η_m = apparent viscosity of complex mixture
η_0 = inherent viscosity without shear (also called consistency index)
m = shear rate sensitivity exponent (also called flow index)

The equation indicates the non-linear relationship between shear stress and shear rate in non-Newtonian rheological behavior, meaning that the apparent viscosity depends upon the shear rate. This behavior is caused by the fact that three-dimensional network 'structures' are present that may break down and rearrange during shear, depending upon the shear rate, particulate concentration and inter-particle forces. Note that emulsion droplets may also deform or coalesce during shear, forming non-spherical or larger droplets. Paint is a good example of the positive effects of the non-linear relationship between viscosity and shear rate of concentrated suspensions during its application. The viscosity should be low enough for good mixing and painting with a brush (when applying a fairly small shear rate), but high enough to remain on the surface without dripping (in the absence of shear). It will be clear that Newtonian flow behavior is characterized by $m = 1$. Several cases can be distinguished (see Fig. 2.2).

Pseudoplastic or shear thinning fluids occur most often (at small shear rates). They show an apparent viscosity that decreases with increasing shear rate (or in Eq. 2.17: $m < 1$). Suspensions of paper pulp and pigments, yoghurt, ketchup, mayonnaise and polymeric solutions (e.g. Xanthan gum) are typical examples. Such behavior occurs when the inter-particle distance is equal to or smaller than the particle size and the particle-particle interactions are medium strong. The resulting three-dimensional network 'structures' break down gradually at increasing shear rates to form two-dimensional arrangements, which have a lower viscosity.

This characteristic is advantageous to processability, stability and applicability of the product (e.g. while mixing or pouring) [3, 4].

Dilatant or shear thickening fluids show an apparent viscosity that increases with increasing shear rate (or in Eq. 2.17: $m > 1$). This behavior indicates that increasing shear rates cause less freedom for movement of the particles, so that fluid flow becomes more difficult. Typical examples are ceramic pastes, (concentrated) suspensions of starch and beach sand. In fact, most products show this behavior at high shear rates, if their particulate concentration is close to maximum packing. High shear rates cause the formation of three-dimensional particle clusters, within which fluid flow is strongly limited. For example, mixing or pumping may require

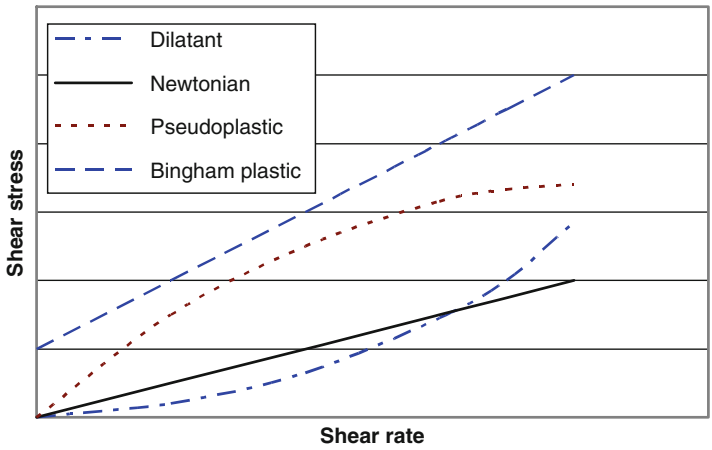

Fig. 2.2 Different types of fluids, where properties are independent of time under shear

much energy or even becomes problematic [3, 85]. Dilatancy, i.e. increase in total volume, often accompanies shear thickening.

Optimum size distributions that promote an increase of maximum particle packing may be investigated to lessen problems (see Sect. 2.5.B) [10, 55, 58, 75]. On the other hand, the same characteristic may be used to improve the performance of composite materials such as shock-absorptive skis and soft body armor [85].

For *Bingham plastic* fluids, such as molten chocolate, aqueous suspensions of rock or clays and sewage sludge, the relating line between shear stress and shear rate does not pass through the origin, since a certain minimum stress (the yield stress) is required to overcome particulate structures. This yield stress is added as a constant to the right hand side of Eq. 2.17 as can be seen in Eq. 2.18:

$$\eta_m = \tau_0 + \eta_0 \left(\frac{d\gamma}{dt}\right)^{m-1} \tag{2.18}$$

At higher shear rates, the relationship between shear stress and shear rate may be linear. Most often, however, Bingham plasticity occurs in combination with shear-thinning or shear-thickening.

The typical viscosity behavior against shear rate – after removal of relaxation and time-dependency – of many concentrated particulate products can be schematically illustrated as in Fig. 2.3 [7, 16, 41].

Typically, four regions can be indicated, for which both the presence and exact structure depends on product composition:

I. Region of zero-shear, Newtonian viscosity (viscosity often typified by η_0)
II. Region of shear-thinning (more or less power law, i.e. linear in double logarithmic plot)

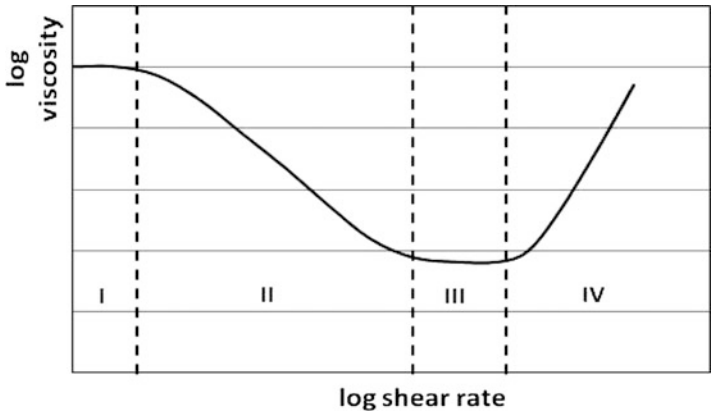

Fig. 2.3 Schematic viscosity – shear rate relationship (relaxation and time-dependency removed)

III. Second region of Newtonian behavior (viscosity often typified by η_∞)
IV. Region of shear-thickening.

Region I corresponds to medium-high particulate concentrations, which – at low shear rates – show no or low dependency of shear rate. In this case, Brownian motion has a dominant influence upon viscosity.

Region II shows shear-thinning behavior, which relates to some kind of alignment of particles. At increasing shear rates, a decrease in viscosity is observed. Here, shear forces between particles dominate the viscosity; this often occurs at high particulate concentrations.

Region III indicates a second period of Newtonian behavior that may occur at high particulate concentrations when shear forces have rearranged the particulate structure to one forming a minimum viscosity.

Finally, region IV corresponds to very high particulate concentrations (near to closest packing). In this state only few particles, or parts of complete particle structures, have the possibility to move. The high shear rate further decrease the possibilities for movement of the mixture.

For some dispersions, the rheological behavior is time-dependent, where behavior depends upon the duration of the shear.

Thixotropic fluids are the first example. They possess a 3-dimensional 'structure' due to inter-particle interactions, which breaks down fairly slowly as a function of time under shear. As a result of this breakdown, shear stress decreases. In other words: the longer the fluid undergoes stress, the lower its viscosity. In the absence of shear, the structure builds up again, which also proceeds fairly slowly. Examples are molten chocolate, some clays, drilling mud and some paints (at high particulate concentrations).

Rheoplastic fluids are the opposite case (also called negative thixotropy). They show an apparent viscosity increase with time when shaken or tapped. Here, some structure builds up during shear. Examples are aqueous sols of bentonite, vanadium pentoxide and gypsum.

In order to obtain typical results in both cases, viscosity measurements are usually executed in steady-state experiments, in which thixotropic effects are counteracted by pretreatment (pre-shearing) of the measurement sample for some (standardized) time period.

Finally, there are *viscoelastic* products. They are intermediate between viscous and elastic products as they show both characteristics [79]. This behavior occurs if the characteristic stress relaxation time τ of the product is comparable to the experimental time t. It can be expressed in terms of the dimensionless Deborah number D_e which relates to both times:

$$D_e = \tau/t \tag{2.19}$$

In case of viscoelastic behavior, D_e equals about 1. Viscous behavior occurs when $D_e << 1$, or $\tau << t$. Elastic behavior is the other extreme; then, $D_e >> 1$, or $\tau >> t$. Elastic objects stretch/deform under stress, but recover their original dimensions when stress is stopped (see a spring as the example). Viscoelastic products, when imposing stress, instantaneously stretch/deform, followed by a slower viscous response. When stress is removed, elastic recovery occurs, followed by a relatively slower (often exponential) viscous recovery. Typically, no full recovery to the initial situation is reached.

Viscoelasticity of products is typically determined through measurement of their response (compliance) in dynamic techniques, viz. from so-called creep curves after sudden application of stress or by oscillatory techniques [79]. The former technique leads to an instantaneous elastic modulus *G(0)*, in addition to a viscous component. Through studying the relaxation after removing the stress, the time-dependency of the elastic modulus G can be evaluated. The response of viscoelastic fluids to oscillatory stress application yields a complex modulus G*, from which the so-called storage (elastic) modulus G' and the so-called loss (viscous) modulus G" can be derived, the latter being the imaginary component of the complex modulus.

Ice cream (cf Chap. 9), blood and polymer solutions are examples of viscoelastic products. An application of viscoelasticity ensures optimum droplet formation from low-viscosity liquids by ink jets. Here, it plays a role by avoiding satellite droplets at high frequencies/speeds [83].

(B). **Particle size distribution**

For concentrated dispersions, the particle size distribution (PSD) influences the rheological behavior in addition to particulate concentration. PSD width and multimodality are important as they are decisive for the maximum packing density of the particles: highest packing densities can be reached in carefully designed multimodal mixtures (see Sect. 2.2). At a given (high) particulate concentration, such increase of the maximum packing density may lead to an enormous decrease of the (apparent) viscosity of the dispersion. This difference between actual and maximum packing density is often used in equations for the rheological behavior (see above). For such concentrated dispersions, steric effects and (temporal) structures of particles as a result of particle-particle interactions play an important

role, especially in liquids of (medium) low viscosity. In general, these interactions relate to the particles' surface area. Thus, the Sauter mean diameter, $D_{3,2}$, is often regarded as the most significant parameter to characterize these relationships. This is especially true if strong electrostatic interactions exist between particles [55].

(C). **Particle shape**

For non-dilute solid concentrations, particle shape influences rheological behavior, as it decreases maximum packing density. The effects increase with increasing aspect ratio and are very important for fibers and plates [55]. For the general case of commercial dispersions, the effects are still significant. Note that emulsion droplets may deform from spherical to elongated shapes, which also influences viscosity.

Given all the possibilities of complex rheological behavior mentioned and the absence of a basic theory, it will be clear that adequate measurements, as well as knowledge and understanding of the influence of particulate characteristics on the behavior, are necessary for good design of products and their production processes. This has become ever clearer, since the complexity of many products has increased significantly over the last decades and thus, composition has become critical. Particle size, size distribution, width and modality, particle shape, zeta-potential, particulate concentration as well as added ingredients play their role. Consequently, the influences on rheological behavior are often highly product-specific. All of these parameters need to be optimized, for rheological behavior as well as for other performance aspects, to reach best products in individual cases.

2.6 Emulsion and Suspension Stability

Industrial emulsions and suspensions are generally required to be stable over an appreciable period of time. This means that sedimentation, flocking, agglomeration, coagulation and coalescence should be prevented. In products, this requires a typical particle size smaller than 1–30 μm, depending on particle density and adequate stabilization. In such cases, sedimentation or creaming is virtually absent. Dispersions containing larger sizes also exist. For these larger particle sizes, high-viscosity liquids, thickening agents or high particulate concentrations usually prevent or limit sedimentation effects. Two stabilizing factors can be distinguished in the general case of dispersions [28, 32, 39, 54, 60, 61]:

(a). Repulsive forces between the particles by electric charges and/or steric hindrance induced at the surface of the particles that prevent particles from coming close together. At high particulate concentrations, when the particles are forced to close proximity, e.g. in pastes, stabilizing structures may result from these repulsive forces.
(b). Brownian motion (particle diffusion), if its velocity is much larger than the rate of settling or creaming (at low particulate concentrations).

Table 2.2 Stability behavior of colloidal dispersions

Zeta-potential, mV	Stability behavior
$< \|10\|$	Rapid coagulation/flocculation
$\|10\|–\|30\|$	Instable
$\|30\|–\|60\|$	Moderate/good stability
$> \|60\|$	Excellent stability

Ionic stabilization of aqueous suspensions results from ionization of hydroxyl or oxide groups at the particle surface. This may be through the influence of the pH, and/or by adsorption of polyvalent ions at this surface. Typically, there is also adsorption of some water molecules in the boundary layer. Emulsions are often stabilized by ionic or non-ionic surfactants. These adsorbed species are strongly bonded to the surface so that they remain attached to the particle as the particle moves. Note that this boundary layer represents a real distance but is conceptual, since the adsorbed species, at some small molecular distance from the true surface, exchange relatively fast with species in the dispersion medium and the surface of shear varies slightly with time and location. Thus, the boundary layer and the surface of shear have a statistical nature. Steric hindrance may give another type of stabilization. It is effective if large polymeric molecules are adsorbed at the surface, which prevent other particles from approaching. Ionic and steric effects are often combined for the stabilization of industrial particulate dispersions. The hydrodynamic particle size – i.e. the particle size at the surface of shear when the dispersed particle is moving in a liquid – is usually somewhat larger than the size of the solid particles as it includes the adsorbed layer of molecules. The differences are typically in the range 1–100 nm, depending on electrolyte concentration and dielectric constant. The electric charge at the shear plane of the moving particle is called zeta-potential (ζ-potential). It is considered to be the relevant parameter for describing the interactions between dispersed particles and the stability of the dispersion. Note that the zeta-potential depends strongly on surface properties of particulate material as well as on the ionic concentration and pH of the dispersion. An increase of the electrolyte concentration of the dispersion fluid, causes a decrease of the zeta-potential. Typical dispersion stability characteristics are provided in Table 2.2 (for aqueous media of low viscosity).

The table shows that long-time stability of dispersions requires a zeta-potential larger than about plus or minus 50 mV, causing strong inter-particle repulsion. A zeta-potential around zero will lead to particle clusters through agglomeration, coagulation or flocculation. A low zeta-potential if often arranged to deliberately induce aggregation and flocculation in order to facilitate filtration or sedimentation. It can also be used in cases that all or specific colloidal particles are to be removed from a dispersion.

Flotation, on the other hand, requires a minimum absolute zeta-potential of about 40 mV. This involves the adsorption of anionic or cationic surfactants (with their polar heads) to convert hydrophilic oxidic particle surfaces, into hydrophobic ones (with their non-polar hydrocarbon tails). This, in turn, facilitates the attachment of air bubbles and, thus, particle removal by flotation attached to the froth formed.

At medium/high particulate concentrations, the above particle interaction effects often cause an increase of the apparent viscosity of a suspension or even some kind of 'structure' for the particulate product, by which means the particles experience a considerable resistance to movement. This resistance is sometimes enlarged by the presence of thickening additives in the mixture (see further Sect. 2.5).

The rate of settling or creaming at viscous flow conditions (i.e. Reynolds number for settling particles < 0.25) in dilute liquid dispersions in relation to particle size is given by Stokes' law [54]:

$$v = \frac{H_s}{t} = \frac{(\rho_P - \rho_L) \cdot g \cdot D_{St}^2}{18 \cdot \eta_L} \tag{2.20}$$

where:

v = terminal settling velocity of a particle
H_s = settling height
t = time for settling over height H
ρ_P = effective particle density[3]
ρ_L = liquid density
g = gravitational acceleration constant
D_{St} = equivalent Stokes' diameter of a particle
η_L = liquid viscosity

This Eq. 2.20 is derived for viscous creep flow conditions, which assume that the drag coefficient C_D is inversely related to Reynolds number Re through:

$$C_D = 24/Re \tag{2.21}$$

The settling rate at higher Reynolds number becomes slower than predicted by Stokes' law through an increased drag force [1]. With an increase in Reynolds number, the relationship between the drag coefficient C_D and the Reynolds number Re becomes more complex. Several approaches for solutions in the 'intermediate' region of $0.25 < \mathrm{Re} < 1{,}000$ have been reported, in the form of both equations and tables.

Concentrated suspensions also cause the sedimentation to become slower than the above velocity predicted by Stokes' law [54]. In this case, the liquid density has to be replaced by an apparent density of the suspension, which relates to the particulate concentration (see further Sect. 2.5). Furthermore, some 'porosity' factor for the solids fraction may have to be added in the equation, which reaches a maximum value of one for dilute suspensions. This 'porosity' factor is analogous to that of powders.

[3] The effective particle density to be used in Stokes' law is best determined by a method where a known weight of dispersed particles displaces a measured volume of suspending liquid. This method regards the influence of pores in the same way as in sedimentation. An absolute density value, determined by gas pyknometer, is not appropriate in the presence of pores.

The Stokes-Einstein equation gives the relation between (hydrodynamic) particle size in colloids and their diffusion coefficient in the absence of particle-particle interaction [54]:

$$\mathbb{D} = \frac{k_B T}{3\pi\eta_L D_h} \tag{2.22}$$

where:

$\mathbb{D}$ = diffusion coefficient
k_B = Boltzmann constant
T = absolute temperature
η_L = liquid viscosity
D_h = (effective) hydrodynamic particle size

In the general case of dilute dispersions of low viscosity, the competition between Brownian motion and sedimentation is decisive for dispersion stability. In aqueous media or other media of low viscosity, Brownian motion typically becomes significant for particle sizes below about 1 μm (assuming particle density is low). In such media, sedimentation becomes very slow below about 0.5 μm. Of course, the exact sizes depend on the density of the particles and the apparent viscosity of the media. Note that attractive or repulsive forces between particles occurring at intermediate or high concentrations may limit Brownian motion significantly.

Many industrial particulate products contain some kind of 'structure' for stabilization, due to their particulate concentration or other reasons. Such 'structures' generally dominate the effects of Brownian motion, creaming and sedimentation (see Sect. 2.5).

For settling of aerosols, Eq. 2.20 is slightly modified [26]:

$$v = \frac{H_s}{t} = \frac{\rho_P \cdot g \cdot C_c \cdot D_{St}^2}{18 \cdot \eta_A} \tag{2.23}$$

In this equation, the relatively small air density is omitted, C_c represents the Cunningham slip correction factor and η_A the air viscosity. C_c accounts for the 'slip' between the particle and the air and reduces the value of the Stokes' drag force. It relates to the Knudsen number and becomes important if the particle size approaches the mean free path of the air molecules. It depends upon both particle size (below about 10 μm) and air pressure. Values for C_c have been tabulated [26].

The aerodynamic particle size (D_{ae}) is commonly used for aerosol particles instead of the Stokes' diameter. It assumes a particle density of 1,000 kg/m^3. Thus:

$$D_{ae} = D_{St} \cdot \sqrt{\rho_P} \tag{2.24}$$

2.7 Color, Opacity, Gloss and Transparency

Visible, white light is composed of light having different colors, which have wavelengths from about 380 nm (violet) to 780 nm (red), named the visible spectrum (see Fig. 2.4). This spectrum can be made visible e.g. by a prism, as refraction depends upon the wavelength (Fig. 2.5). In a rainbow, it is caused by refraction of sunlight through the rain drops. In this spectrum, there are three so-called primary colors, viz. blue, green and red. Other colors are formed by combination of these three, as we learn as children when we start producing colored drawings (Fig. 2.6). Note that the human perception of colors depends upon the relative spectral sensitivity of the cones in the retina of our eyes, the so-called luminous efficiency function.

Many materials have the property of absorbing light at specific wavelengths, where the unabsorbed fraction of the incident light is transmitted or reflected. Thus, these materials appear to be colored. The same phenomenon causes these materials to give another color impression if the spectrum of light, falling upon them, for example from public lighting at night, differs from sunlight. Color may be regarded as an impression of the combined intensities of light at different wavelengths, reaching our eyes and interpreted by our brain.

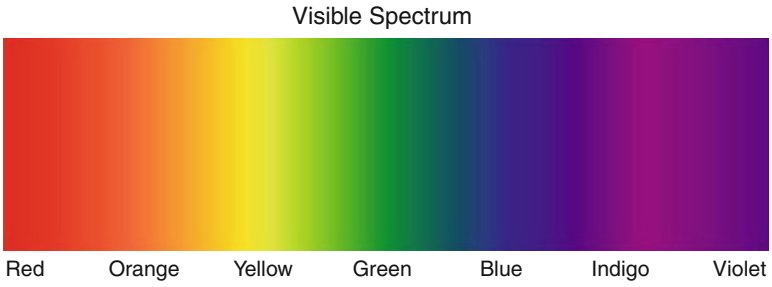

Fig. 2.4 Visible spectrum

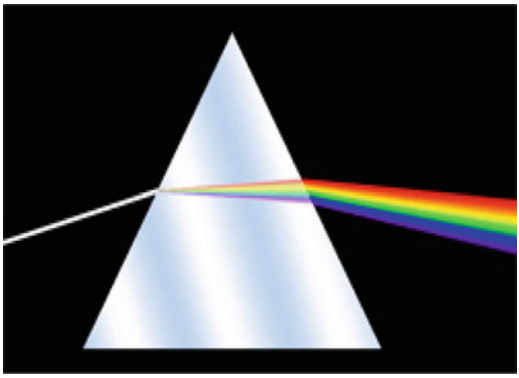

Fig. 2.5 Refraction of white light in a prism

Fig. 2.6 Color composition

There are two types of colorant substances, viz. dyes and pigments. Dyes are soluble in the substrate, in which they are dispersed; pigments are insoluble. Both types are typically used to improve the esthetic appeal of objects. The colorant effect of dyes comes from molecular structure, viz. the number of conjugated double bonds. The color of pigments is primarily governed by their chemical composition and crystal structure (see also Chap. 12). These properties determine the refractive index of the particles and, thus, their absorption, reflection and scattering at the different wavelengths of visible white light. Particle size and shape are important as well, in view of their relationship to the degree of scattering of light by the particles [50, 54].

The effects of light absorbance in relation to concentration and path length are quantified in the equation of Beer-Lambert-Bouguer:

$$A = \ln(I/I_0) = \varepsilon_\lambda \cdot c \cdot l \tag{2.25}$$

where

A = absorbance (or light extinction)
I_0 = intensity of incident light of given wavelength
I = intensity of transmitted light at given wavelength
ε_λ = molecular extinction coefficient (at a given wavelength)
c = concentration
l = path length

The gloss of surfaces is related to a uniform reflection of light (angle of incoming light equals angle of reflected light; parallel rays in cause parallel rays out). Rough surfaces or the presence of particles or pores causes reduction of gloss (matting) as the reflection becomes more diffuse.

The opacity of pigments is caused by light scattering and absorption by the composing surface molecules and/or optical heterogeneities (e.g. particles). For e.g. white paints, containing small TiO_2 particles, light scattering is the dominant

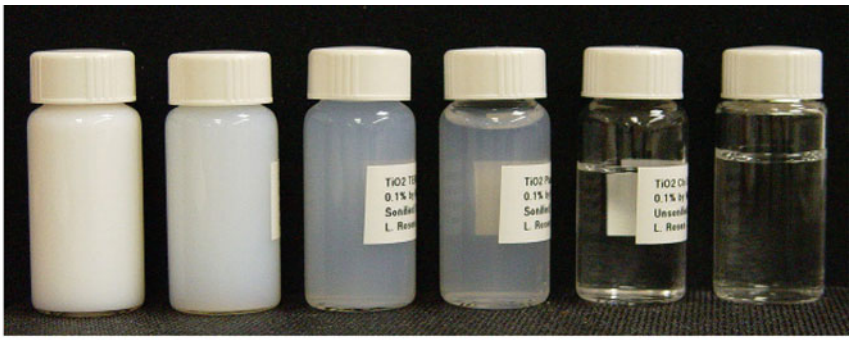

Fig. 2.7 Influence of TiO_2 particle size on turbidity (0.1 % w/w in water) [68]

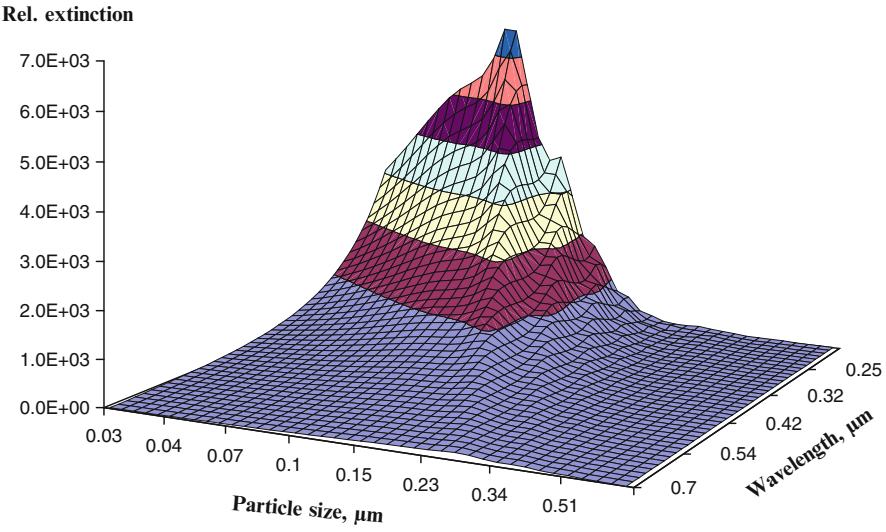

Fig. 2.8 Relative extinction for equal volumes of particles of different size; particle RI = 2.4 – 0 i, in water RI = 1.33. Courtesy M. Wedd

cause for opacity (see also Chap. 12). At the optimum particle size (for rutile about 200–300 nm), the scattering efficiency (ratio of optical cross section to actual particle cross section) is about 5, against about 2 for larger particles than about 10 µm. For particles smaller than about 100 nm, the scattering power decreases with the 6th power of particle size. The scattering power of particles also relates to the inverse of wavelength to the 4th power. Therefore, scattering power strongly increases with decreasing wavelength. This assists some dispersions to become fairly or even fully transparent at visible wavelengths but permit absorption of the dangerous UV wavelengths as needed for sunscreens. Figure 2.7 nicely illustrates the influence of particle size on turbidity for aqueous TiO_2 dispersions. Such very small particle sizes may be attractive in e.g. sunscreens (see Chap. 14). Figure 2.8

exemplifies the relative extinction at different wavelengths for equal volumes of particles having different sizes in suspension (at RI of particles = 2.4). Note that particle volume relates to the cube (3rd power) of particle size.

Particle size and shape affect the quality of e.g. paint and sunscreen in tinting strength, hiding power and transparency. And at low particle concentration, the scattering differences are used in both the laser diffraction and the ultrasound extinction technique for measurement of particle size distributions.

Computer codes have been derived for calculation of scattering matrices that describe the angular light scattering patterns of spheres in relation to their size and optical properties. Various theories are used as basis for these codes. Mie theory is the general theory. It describes the general relationship between the particle size of spheres, refractive index of the particles, the wavelength of the light source, the angular pattern of scattered light intensities, and the scattering efficiencies for each size. Rayleigh theory is also used but is limited to particles smaller than about 100 nm. It assumes particles to be point sources and calculates that the scattered light intensities decrease with the 6th power of particle size (thus, 2nd power per unit of volume of such particles) and are equal in all directions. Fraunhofer theory is exclusively based upon the diffraction at the particle contours and is an approximation that is generally valid for particles larger than about 50 μm, though fully opaque particles allow a lower limit (down to about 2 μm). Its main advantage is that it does not require values for the refractive index and that it allows for much simpler calculations [54] at the cost of reduced accuracy of the quantity of small particles. Most computer codes for light scattering calculations are limited to low concentrations of spherical particles, since they assume that light is scattered only once by a particle (single scattering). When the concentration is increased, the scattered light may be scattered again by other particles (multiple or diffuse scattering). The fine-structure of the scattering patterns decreases by the presence of particles of different size as well as by multiple scattering. As a consequence, calculations become increasingly complex. Modern computers, however, have proven to be capable of performing such calculations through using e.g. so-called T-matrix codes for evaluation of the basic Maxwell equations [56, 57, 89]. These codes can also be used for calculation of scattering patterns of non-spherical and heterogeneous particles.

In order to reach the desired color and hiding power for e.g. paint applications, pigments are usually mixed. The equations given by Kubelka-Munk and Duncan are often used in the design of such mixtures.

Both color and opacity can be derived from the measured diffuse reflectance curves with respect to wavelength, through the Kubelka-Munk theory [24, 27, 38, 43, 44]:

$$\left(\frac{K}{S}\right)_{\lambda} = \frac{\left(1 - R_{\lambda,\infty}\right)^2}{2R_{\lambda,\infty}} = f(R) \tag{2.26}$$

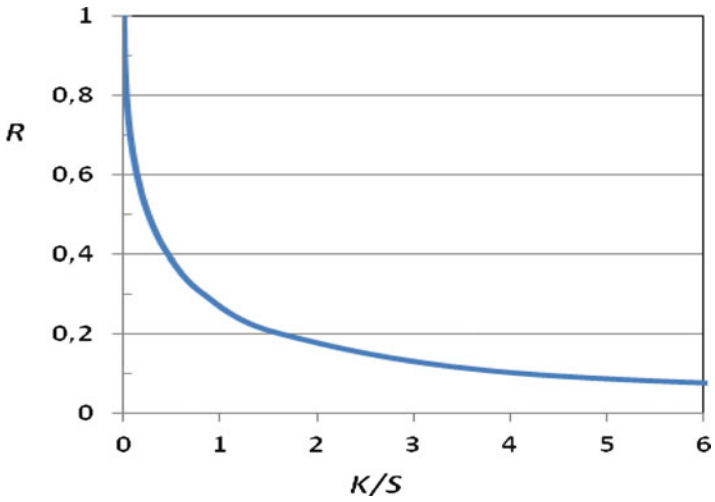

Fig. 2.9 Relationship between R and K/S

where:

K = absorption coefficient of the K-M theory
S = scattering coefficient of the K-M theory
$R_{\lambda,\infty}$ = measured reflectance at given wavelength and infinitely thick layer
λ = wavelength

Although the theory has a phenomenological origin, its absorption and scattering coefficients were later proven to relate to the single-scattering and extinction coefficients. ln K is twice the extinction coefficient of the Beer-Lambert-Bouguer equation (Eq. 2.25), even at high pigment concentrations. S has a more complex relationship with the Mie scattering coefficient, since it also depends on pigment concentration [38, 59, 62, 67].

The K-M equation is quite helpful since its results, illustrated in Fig. 2.9, inform us that reflectance will decrease at increasing K/S, for example if we add a strongly absorbing pigment such as carbon black to the system. On the other hand, reflectance increases if we increase S/K, e.g. by addition of a strongly scattering white pigment.

As illustrated above, pigments are most often used in combinations to provide the required color and hiding power. Duncan has demonstrated that the contributions of scattering and absorption by individual constituents in a mixture can be summed [12, 27, 38]:

$$\left(\frac{K_{mix}}{S_{mix}}\right)_{\lambda} = \left(\frac{c_1K_1 + c_2K_2 + c_3K_3 + ...}{c_1S_1 + c_2S_2 + c_3S_3 + ...}\right)_{\lambda} \tag{2.27}$$

Equation 2.27 is often used to design color as well as hiding power of pigment mixtures.

The desired color is the result of mixing various colored pigments at appropriate concentrations, with the hiding power achieved through the addition of white pigment (see further Chap. 12).

Pigment application for hiding power is most effective when particle size is about half the dominant wavelength of the light (about 200–400 nm); then, a least amount of pigment is required for the given task of protection and obliterating the color of the substrate. Particle size for maximum hiding power for spheres having a high RI can be calculated with the approximating equation given by Weber [86]:

$$D_{scmax} = \frac{2\lambda}{\pi(n_P - n_L)} \tag{2.28}$$

where:

D_{scmax} = particle size at maximum scattering power
λ = wavelength incident light
n_P = refractive index particle
n_L = refractive index liquid

For transparent applications, much smaller particles – in the nano-size range – are used; these have much less capacity for scattering light (see above, Rayleigh theory and Figs. 2.7 and 2.8). Nano-particles may also be used for catalytic applications, where maximum catalytic surface area per unit mass is desired.

2.8 Sensorial Characteristics

Sensorial characteristics are important in our human appreciation of foods, sweets, beverages and cosmetics [18, 40, 73, 78]. Taste, for example, relates to a combination of aroma, texture, odor, visual and auditive characteristics more or less independent of product type (solid, semi-solid or fluid) and use. Bitter, salt, sour, sweet and umami (savoury) are presently considered as the five basic tastes [29, 47]. Some examples of popular terminology in relation to specific products are presented in Table 2.3. A lexicon of terms and definitions has been published by ASTM [2].

Most consumer products of this kind consist of two or more phases. The sensorial properties have both psychological and physical aspects. The terminology is semi-quantitative. The psychological aspects are individual. For example, some people like bitter chocolate, others like milk chocolate. Sense of taste also depends to some extent on the country of origin culture, for example appreciation or dislike of some special kinds of vegetables, cheeses or spice. Physical aspects can be subdivided in mechanical, geometrical and other characteristics, in addition to aroma. Mechanical aspects correspond to some kind of texture, geometrical ones to the particulate nature.

A wide variety of causes may influence the physical characteristics of products such as rheological behavior, chewiness, etc. Particle size and size distribution

Table 2.3 Examples of popular terminology for taste characteristics in products

Product type	Characteristics	Product examples
Solid	Crisp, brittle, crumbly, powdery Creamy, gritty, grainy, coarse Tender, chewy, tough, plastic Moist, dry, sticky, soggy	Apples, biscuits, carrots, chocolate, cornflakes, gum, meat, sweets
Semi-solid	Pasty, mealy, coherent Moist, dry, sticky, soggy Lumpy, smooth	Butter, cheese, creams, fish, margarine
Fluid	Thin, watery, viscous Creamy, fatty, greasy Sticky, tacky Bubbly, tingly	Beverages, margarine, mayonnaise, milk, soups

(of solid, liquid and air 'particles' dispersed in another phase), particle shape and particulate concentration are important geometrical aspects. The type and melting range of the ingredients (in relation to temperature of the environment or the human body), moisture content, etc. are included in other aspects. Note that the particle size and shape of ingredients may influence the sensorial properties of a product in addition to its processability (rheological behavior).

Specific products may show different or similar relationships between particle characteristics and performance. For example, they might wish to limit the degree of grittiness in our mouths, which depends on product composition and temperature. In chocolate we experience a change in mouth-feel from creamy to gritty when the $D_{90;3}$ of the sugar particles increases from about 20 to 30 μm and in ice cream above about 55 μm [30]. Over these size ranges, we are able to sense some individual solid particles in between our finger tips. Other similar effects are the influence of particle size on e.g. powder flow and suspension viscosity (see Sects. 2.3 and 2.5).

In view of its complex nature, taste is generally tested by trained panels, which use standard procedures and terminology [88]. Often, these tests are combined with measurements of e.g. viscosity, elasticity, hardness, turbidity, etc.

2.9 Adsorption and Catalysis

Porosity and pore size distribution of particles are essential factors for their ability to act as adsorbents, catalysts or ion exchangers in industrial processes. On the one hand, wide pores favor quick access and removal of components. On the other hand, narrow pores provide for a large surface area for adsorption or reaction. The minimum pore width for a given application is defined by the size of the molecules involved. Pore sizes are classified into three categories, viz. [74]:

- Macropores, with pore diameters larger than 50 nm
- Mesopores, with pore diameters in the range 2–50 nm
- Micropores, with pore diameters smaller than 2 nm.

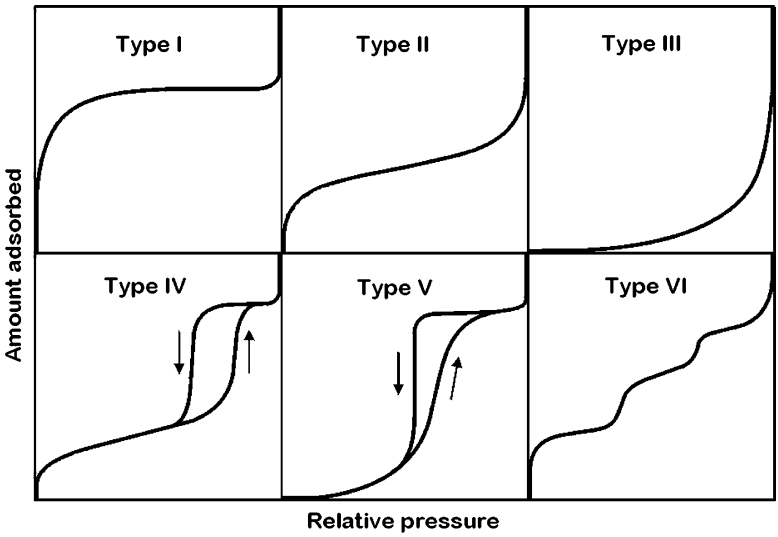

Fig. 2.10 Types of physisorption isotherms

Note that the size of many voids in between particles is in the same order of magnitude as the size of the particles. Although voids are usually larger than pores, some overlap in size occurs due to the irregular shape of the voids.

Mercury penetration and gas adsorption techniques (using physisorption with physical attractive forces between adsorbent and adsorbate) are most often used for determination of pore size distributions and specific surface area (see also Chap. 3). Mercury penetration technique employs the pressure required for the penetration of mercury into the pores and voids as a measure of pore size. The inverse relationship between pressure and pore size requires that higher pressures are needed for smaller pores/voids (see also Chap. 3).

In the gas adsorption technique, the amount of adsorbate for a known amount of adsorbent is determined at various relative pressures (P/P_0). For characterization, nitrogen is often used as adsorbate and measurement takes place at its boiling point temperature of about – 196 °C (77 K). For most adsorbates, the majority of physisorption isotherms may be grouped into six types, as shown in Fig. 2.10 [31, 33–35, 74]:

Type I isotherms show a limiting value at increasing relative pressures. This is reversible and typical for microporous solids, where the sorption is limited by the accessible micropore volume rather than the internal surface area.

Type II isotherms are also reversible and the normal form for non-porous and macroporous adsorbents. They represent unrestricted monolayer-multilayer adsorption. Within the relative pressure range of about 0.25–0.35 there is a point at which monolayer coverage is nearly complete and multilayer adsorption is about to begin. This is usually regarded to be the end point for application of the BET equation for surface area measurement (see Chap. 3).

Type III isotherms are also reversible and typical for systems where adsorbate-adsorbate interactions play a more important role than adsorbent-adsorbate interactions. This type is not common.

Type IV isotherms are the most common form for mesoporous sorbents. The initial part of the isotherm is attributed to monolayer-multilayer adsorption (as in type II), but at higher relative pressures they show a hysteresis loop, which is associated with capillary condensation in the mesopores. Different shapes of the hysteresis loops can be related to different specific pore structures. Similar to type II isotherms, relative pressures up to about 0.35 are used for surface area measurement (see Chap. 3).

Type V isotherms are typical for weak adsorbent-adsorbate interactions. They are uncommon and show relationship to type III isotherms.

Type VI isotherms show a stepwise increase of adsorbate at increasing relative pressures and are also uncommon. The step height represents the monolayer capacity for each adsorbed layer. The steps show stepwise multilayer adsorption, onto a uniform non-porous surface.

Within the measurement techniques for pore size distributions (cf. Chap. 3), a cylindrical pore shape is generally assumed. Other types of idealized pore shapes used are e.g. ink bottle pores (having a restricted opening), slit-shaped pores and wedge-shaped pores. In practice, however, pores often have an irregular shape.

Processes that include adsorption, catalysis and ion exchange, are governed by the presence of both specific chemical elements or groups and a large specific surface area. Specificity is often favored by using a specific particular pore architecture for connecting different pore sizes.

Adsorption occurs by physical attractive forces (physisorption), but specific chemical bonding may occur as well (e.g. between carbon monoxide and platinum; chemisorption). In industrial applications, adsorbents are typically applied to remove water or hazardous components from flue gas, waste water or process water (e.g. sulphur dioxide or sulphate). Specificity may be obtained by using adsorbents with a specific pore size, which limits entrance of the large species present. This is, for example, used in the separation of normal and branched paraffins in molecular sieves, where the former can enter the pores and the latter cannot (‘molecular sieving phenomenon’).

Ion exchange is used to remove ions that are considered to harm a process or the environment (e.g. calcium or heavy metals). It requires the presence of specific, harmless ions (e.g. sodium) at the surface that can be exchanged with the harmful ions. Here too, some specificity can be obtained by using ion exchangers with a specific pore size, which favors entrance of the targeted ions.

Catalysis is a very complex process. It requires adequate adsorption of several reactants onto a surface as well as the ability of that surface to catalyze the rapid and selective conversion into the desired components. Solid catalysts require a large surface area of catalytic material (usually a highly dispersed metal on a large inert surface) as well as rapid access of reactants and rapid removal of produced components. Catalytic reactions are sometimes executed in fluid beds, sometimes

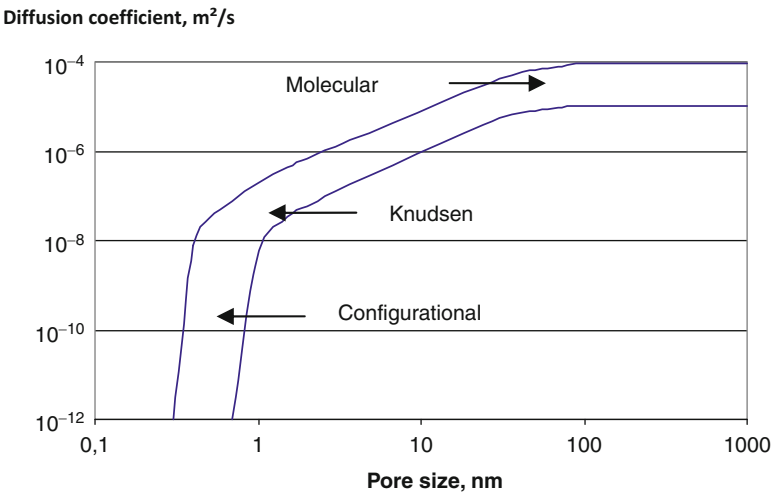

Fig. 2.11 Schematic of gas diffusion regions in pores

in fixed beds. Adequate behavior of the catalysts requires adequate engineering of particle size, pore size distribution and architecture in relation to the molecular size of all components involved.

The specific surface area of porous particles, is usually established from a gas adsorption measurement, at the point where a monolayer of adsorbed gas may be assumed (see above and Chap. 3). It includes any internal surface of pores. Specific surface area lies within the range of 100–1,000 m^2/g for porous particles. For non-porous, spherical particles, it inversely relates to particle size:

$$S = \frac{6\pi \cdot D^2}{\pi \cdot D^3 \cdot \rho} = \frac{6}{D \cdot \rho} \tag{2.29}$$

where:

S = specific surface area
D = spherical particle diameter
ρ = true particle density

From this equation it can be easily derived that solid, non-porous spheres with diameters in the range of 0.1–10 μm have a specific surface area of about 60–0.6 m^2/g. The above quoted value of 100 m^2/g is only reached for solid particles smaller than about 50 nm (calculated for unit density of 1,000 kg/m^3).

Diffusion (Brownian motion) is the driving force for transport of molecules in pores [11, 42]. Besides temperature, the effective molecular size, the pore size and adsorption determine the possibilities and the rate of transport. Four diffusion mechanisms can be distinguished in the following schematic way, which may act in conjunction (cf. Fig. 2.11).

- *Molecular diffusion* (also called *bulk or Fick diffusion)* occurs when the pore diameter is large in comparison to the mean free path length of the molecules. Molecules will diffuse independently of pore size at a rate related to their diffusion coefficient, which is inversely related to molecular size. Small molecules diffuse faster than larger ones. Generally, diffusion coefficients are in the range 10^{-4}–10^{-5} m^2/s.
- *Knudsen diffusion* prevails, when the mean free path length of the molecules is fairly large in comparison to the pore diameter. Frequent collisions of the molecules with the pore wall retard diffusion. The Knudsen diffusion coefficients are proportional to the pore diameter and inversely proportional to molecular weight of the diffusing component. Their value is generally in the range 10^{-5}–10^{-7} m^2/s.
- *Activated, configurational diffusion* occurs when the size of the molecules is almost the same as the pore diameter. Strong interaction between molecules and pore wall result in very slow transport. Generally, diffusion coefficients are smaller than 10^{-8} m^2/s.
- *Surface diffusion* is possible, when the molecules have a greater tendency for adsorption. In this case, transport mainly takes place in the 'liquid' adsorbate layer, which may strongly enhance diffusional flux in comparison to both Knudsen and configurational diffusion.

Note: Molecules, of course, cannot enter pores when they are larger than the pore size.

2.10 Definitions, Abbreviations and Symbols

Adsorbate	Enriched adsorptive at the surface of the adsorbent
Adsorbent	Solid that adsorbs the adsorptive
Adsorption	Enrichment of the adsorptive at a solid surface
Adsorptive	Gas or vapor (or a specific liquid component) to be adsorbed
Agglomerate	Assemblage of primary particles with intermediate attractive forces (sometimes named aggregate)
Agglomeration	Formation of agglomerates
Aggregate	Assemblage of primary particles with strong attractive forces (sometimes named agglomerate)
Aspect ratio	Ratio of maximum to minimum Feret diameter of a particle (in some literature, the inverse is used, i.e. ratio of minimum to maximum Feret diameter)
Coagulation	(active) formation of (large) agglomerates, often by addition of electrolyte or other specific chemical to a suspension
Coalescence	Collision of droplets in an emulsion, followed by merging to a larger droplet
Cohesivity	Stickiness of a powder, caused by strong attractive and/or frictional forces between individual particles
Colloid	Dispersion of particles having a size range of about 1 nm – 1 μm in a liquid

(continued)

(continued)

Cumulative size distribution	Distribution of the fraction of material smaller (undersize) or larger (oversize) than given particle sizes against particle size
Effective powder density	Density of powder bed measured at well defined conditions
Effective particle density	Particle density measured at well defined, optimum conditions for dispersion in a liquid that includes effects of any retained gas or liquid within the closed or open pores of the particle
Equivalent sphere	Sphere that has the same property as the observed particle in relation to a given measurement principle
Floc	Assemblage of loosely bound primary particles in a liquid
Flocculation	Formation of flocs, usually intentional by addition of a specific flocculation aiding chemical
Median size	Particle size at the point in a cumulative size distribution, where 50 % of the particles is smaller and 50 % larger
Particle size	Diameter of some defined equivalent sphere
Pore	Cavity or channel within an object, such as a particle
Powder bed porosity	Void fraction in the powder bed (packed or fluidized)
Principal component analysis	Mathematical procedure for resolving large data sets into orthogonal components, whose linear combinations approximate the original data to any desired degree of accuracy
Shear stress	Type of stress resulting from shear forces, coplanar with a material cross section
Strain	Deformation of a body due to stress
Stress	Force within a deformable body as a reaction to an external force (often also used for the external force)
Umami	Fifth basic taste (brothy, savory), imparted by glutamate and ribonucleotides [29, 47]
Void	Space between particles, usually in a powder
Zeta potential	electrostatic potential at the layer of shear of a particle suspended in a liquid
IFPRI	International Fine Particle Research Institute
ISO	International Standards Organisation
IUPAC	International Union of Pure and Applied Chemistry
PSD	Particle size distribution
a	Powder packing factor (depends on way of packing)(Eq. 2.2)
b	Particle shape factor for packing equation (Eq. 2.2)
c_1, c_2, c_3	Proportionality constants of an estimated polynomial (Eq. 2.15)
C_D	Drag coefficient
CI	Carr Compressibility Index (Eq. 2.4)
D	Particle size (diameter of equivalent sphere)
$D_{3,2}$	Sauter mean diameter, area-weighted mean size, mean value of surface area-weighted PSD
$D_{50;3}$	Median particle size of volume-based size distribution
$D_{90;3}$	90th percentile of cumulative, volume-based particle size distribution
D_{ae}	Aerodynamic particle size of aerosol particles
D_h	(Effective) hydrodynamic particle size
D_{St}	Equivalent Stokes' diameter of a particle
$\mathbb{D}$	Diffusion coefficient
g	Gravitational acceleration constant

(continued)

(continued)

H	Hausner Ratio (Eq. 2.5)
H_s	Settling height
H_b	Bed height
k_B	Boltzmann constant
K	Resistance constant depending on channel geometry (Eq. 2.7)
L	Length of capillary
m	Shear rate sensitivity exponent (also called flow index) (Eq. 2.17)
M	Mass of powder bed
p	Powder packing exponent (depends on way of packing) (Eq. 2.3)
P	Actual pressure
P_0	Saturation pressure
ΔP	Pressure drop over bed or tube
$r_{i,j}$	Ratio of equivalent packing sizes between components i and j of a bimodal mixture (Eq. 2.3)
$R_{i,j}$	Ratio of equivalent volume diameters between components i and j of a bimodal mixture (Eq. 2.3)
Re	Reynolds number
S	Specific surface area
t	Time for settling over height H_s
T	Absolute temperature
u_s	Linear fluid velocity
$<u_s>$	Mean linear superficial fluid velocity
v	Terminal settling velocity of a particle
V_B	Volume of powder bed
V_f	Freely settled volume per unit mass of powder
V_P	Volume of particles in bed
V_t	Tapped volume par unit mass of powder
V_V	Volume of voids
$(d\gamma/dt)$	Shear strain rate (or shear rate)
ε	Powder bed porosity (void fraction in powder bed)
ε_{fl}	Void fraction during fluidization
ε_0	Limiting porosity (in either tap density or some apparent density)
η_d	Viscosity of dispersion
η_F	Fluid viscosity
η_L	Viscosity of liquid (Newtonian)
η_m	Apparent viscosity of complex mixture
η_0	Inherent viscosity without shear
η_{rel}	Relative viscosity
Φ	Effective volume fraction of dispersed phase
Φ_v	Volumetric flow rate
ρ	True particle density
ρ_B	Effective bulk density
ρ_e	Envelope particle density (including all intra-particle pores)
ρ_f	Freely settled bulk density of powder
ρ_F	Density of fluid
ρ_L	Liquid density
ρ_P	Effective particle density
ρ_t	Tapped bulk density of powder
τ	Shear stress (force per unit area)

References

1. Allen, T.: Powder Sampling and Particle Size Determination. Elsevier, Boston (2003)
2. ASTM DS72: Lexicon for Sensory Evaluation of Aroma, Flavor, Texture and Appearance. American Society for Testing and Materials, Philadelphia (2011)
3. Barnes, H.A.: Shear-thickening ("Dilatancy") in suspensions of nonaggregating solid particles dispersed in newtonian liquids (review). J Rheol. **33**(2), 329–366 (1989)
4. Barnes, H.A.: Thixotropy – a review. J. Non-Newtonian Fluid Mech. **70**, 1–33 (1997)
5. Behringer, R., Louge, M., McElwaine, J., Mort, P., Pfeffer, R., Sundaresan, S.: Report of the IFPRI owder flow working group SAR30-08 (2005)
6. Brinkmann, H.C.: The viscosity of concentrated suspensions and solutions. J. Chem. Phys. **20**, 571 (1952)
7. Caldwell, D.H., Babbitt, H.E.: Flow of muds, sludges and suspensions in circular pipe. Ind. Eng. Chem. **33**, 249–256 (1941)
8. Carman, P.C.: Fundamental principles of industrial filtration. Chem. Eng. Res. Des. **16a**, 168–188 (1938)
9. Carr, R.L.: Evaluating flow properties of solids. Chem. Eng. **72**, 163–168 (1965)
10. Cheng, D.C.H., Kruszewski, A.P., Senior, J.R., Roberts, T.A.: The Effect of particle size distribution on the rheology of an industrial suspension. J. Materials sci. **25**, 353–373 (1990)
11. Coulson, J.M., Richardson, J.F., Backhurst, J.R., Harker, J.H.: Chemical Engineering, vol. I, Fluid Flow, Heat Transfer and Mass Transfer. Butterworth-Heinemann (1999)
12. Duncan, D.R.: The identification and estimation of pigments in pigmented compositions by reflectance spectrophotometry. J. Oil Color Chem. Assoc. **45**, 300–324 (1962)
13. Eilers, H.: Die Viskosität von Emulsionen Hochviskoser Stoffe als Funktion der Konzentration. Kolloid Zeitschrift **102**, 154–169 (1943)
14. Einstein, A.: Investigations on the Theory of Brownian Movement. Dover Publications, New York (1956)
15. Einstein, A. Ann. Physik Lpz. **19** (1906) 289 and **34** (1911) 591
16. Eley, R.R. In: ASTM Paint Testing Manual, pp. 333–368. ASTM Internat (1995)
17. Emery, E., Oliver, J., Pugsley, T., Sharma, J., Zhou, J.: Flowability of moist pharmaceuticals. Powder Technol. **189**, 409–415 (2009)
18. Engelen, L., van der Bilt, A.: Oral physiology and texture perception of semisolids. J. Text. Studies **39**, 83–113 (2008)
19. Farris, R.J.: Prediction of the viscosity of multimodal suspensions from unimodal viscosity data. Trans. Soc. Rheol. **12**, 281–301 (1968)
20. Geldart, D. (ed.): Gas Fluidization and Technology. Wiley, New York (1986)
21. Geldart, D. In: McGlinskey, D. (ed.), Characterization of Bulk Solids. Oxford, CRC-Blackwell (2005)
22. German, R.M., Park, S.J.: Handbook of Mathematical Relations in Particulate Materials Processing. Wiley, Hoboken (2008)
23. Green, D.W., Maloney, J.O. (eds.): Perry's Chemical Engineers Handbook. McGraw-Hill, New York (1984)
24. Hammond III, H.K., Kigle-Boeckler, G.: Gloss. In: ASTM Paint Testing Manual. ASTM International (1995)
25. Hiemenz, P.C., Rajagopalan, R.: Principles of Colloid and Surface Chemistry. Marcel Dekker, New York (1997)
26. Hinds, W.C.: Aerosol Technology: Properties, Behavior and Measurement of Airborne Particles. Wiley, New York (1999)
27. Howell, D.M.: The technology, formulation and application of powder coatings; series in surface coatings technology. In: Sanders, J.D. (ed.), vol. 1. Wiley, New York (2000)
28. Hunter, R.J.: Zeta Potential in Colloid Science; Principles and Applications. Academic, New York (1981)

29. Ikeda, K.J.: New seasonings. Tokyo Chem. Soc. **30**, 820–836 (1909) (Japanese); English translation in: Chem. Senses **27** (2002) 847–849
30. Imai, E., Saito, K., Hatakeyama, M., Hatae, K., Shimada, A.: Effect of physical properties of food particles on the degree of graininess perceived in the mouth. J. Text. Studies **30**, 59–88 (1999)
31. ISO 9277.: Determination of the Specific Surface Area of Solids by Gas Adsorption Using the BET Method; (in revision) International Standards Organisation (1995)
32. ISO 13099 (in prep.).: Methods for Zeta Potential Determination; International Standards Organisation
33. ISO 15901-1.: Evaluation of Pore Size Distributions of Solid Materials by Mercury Porosimetry. International Standards Organisation (2005)
34. ISO 15901-2.: Evaluation of Pore Size Distributions of Solid Materials by Gas Adsorption (and corrigendum). International Standards Organisation (2006/2007)
35. ISO 15901-3.: Analysis of Micro-pores by Gas Adsorption. International Standards Organisation (2007)
36. Jenike, A.W.: Gravity flow of bulk solids. Utah. Eng. Exp. Stn. Bull. **108**, 1–294 (1961); Univ. Utah, Salt Lake City
37. Jenike, A.W.: Storage and flow of solids. Utah. Eng. Exp. Stn. Bull. **123**, 1–194 (1964); Univ. Utah, Salt Lake City
38. Johnston, R.M.: Color theory (Ch. III-D-b). In: Patton, T.C. (ed.), Pigment Handbook, vol. III, Characterization and Physical Relationships. Wiley, London (1973)
39. Kissa, E.: Dispersions: Characterization, Testing and Measurement. Marcel Dekker, New York (1999)
40. Kramer, A., Szczesniak, A.S.: Texture Measurements of Foods. D. Reidel, Dordrecht (1973)
41. Krieger, I.M., Dougherty, T.J.: A mechanism for non-newtonian flow in suspensions of rigid spheres. Trans. Soc. Rheol. **3**, 137–152 (1959)
42. Krishna, R.: A unified approach to the modelling of intraparticle diffusion in adsorption processes. Gas Separ. Purif. **7**, 91–104 (1993)
43. Kubelka, P., Munk, F.: Ein Beitrag zur Optik der Farb Anstriche. Zeitschr. f. techn. Physik **12**, 593–601 (1931)
44. Kubelka, P.: New contributions to the optics of intensely light - scattering materials, Part I. J. Opt.Soc. Am. **38**, 448–457 (1948)
45. Lavoie, F., Cartilier, L., Thibert, R.: New methods characterizing avalanche behavior to determine powder flow. Pharm. Res. **19**, 887–893 (2002)
46. Lee, Y.S.L., Poynter, R., Podczek, F., Newton, J.M.: Development of a dual approach to assess powder flow from avalanching behavior. AAPS PharmSciTech. **1** (2000) art. 21
47. Lindemann, B., Ogiwara, Y., Ninomiya, Y.: The discovery of Umami. Chem. Senses **27**, 843–844 (2002)
48. Lyklema, J. (ed.): Fundamentals of Interface and Colloid Science. Particulate Colloids, vol. IV. Elsevier, London (2005)
49. Macosco, C.W.: Rheology: Principles, Measurement and Applications. VCH Publishers, New York (1994)
50. Marrion, A.: The Chemistry and Physics of Coatings. Royal Soc. Chem, Cambridge (2004)
51. Masuda, H., Higashitani, K., Yoshida, H.: Powder Technology; Fundamentals of Particles, Powder Beds and Particle Generation. CRC Press, Boca Raton (2007)
52. McGee, E.: Predicting powder flow. Pharm. Tech. (June, 2007)
53. McGlinskey, D. In: McGlinskey, D. (ed.), Characterization of bulk solids. CRC-Blackwell, Oxford (2005)
54. Merkus, H.G.: Particle Size Measurements; Fundamentals, Practice, Quality. Springer, Dordrecht (2009)
55. Metzner, A.B.: Rheology of suspensions in polymeric liquids. J. Rheol. **29**, 739–775 (1985)
56. Mischenko, M.I., Travis, L.D., Lacis, A.A.: Scattering, Absorption and Emission of Light by Small Particles. Cambridge Univ. Press, New York (2002)
57. Mischenko, M.I., Travis, L.D., Lacis, A.A.: Multiple Scattering of Light by Particles: Radiative Transfer and Coherent Backscattering. Cambridge Univ. Press, New York (2006)

58. Mongia, G., Ziegler, G.R.: The role of particle size distribution of suspended solids in defining the flow properties of milk chocolate. Int. J. Food Prop. **3**, 137–147 (2000)
59. Mudgett, P.S., Richards, L.W.: Multiple scattering calculations for technology. Appl. Optics **10**, 1485–1502 (1971)
60. Nelson, R.D.: Dispersion of powders in liquids. In: Kirk-Othmer Encyclopedia of Chemical Technology, vol. 19. Wiley, Chichester (1996)
61. Nelson, R.D.: Dispersion of Powders in Liquids. Elsevier, New York (1988)
62. Phillips, D.G., Billmeyer Jr., F.W., Coatings, J.: Predicting Reflectance of Color and Paint Films; IV Kubelka - Munk Scattering Coefficient. J. Coatings Technol. **48**[616], 30–36 (1976)
63. Qi, F., Tanner, R.I.: Random close packing and relative viscosity of multimodal suspensions. Rheol. Acta, 04 Oct. **2011** (online)
64. Rhodes, M.: Introduction to Particle Technology. Wiley, Chichester (1998)
65. Riley, F.L.: Structural Ceramics; Fundamentals and Case Studies. Cambridge Univ. Press, New York (2009)
66. Roscoe, R.: The viscosity of suspensions of rigid spheres. Brit. J. Appl. Phys. **3**, 267–269 (1952)
67. Schabbach, L.M., Bondioli, F., Ferrari, A.M., Petter, C.O., Fredel, M.C.: Colour in ceramic glazes: Efficiency of the Kubelka - Munk model in glazes with a black pigment and opacifier. J. Eur. Ceram. Soc. **29**, 2685–2690 (2009)
68. Scott, D.M.: Improving control of particulate processes via ultrasonic spectroscopy. In: APACT10: Advances in Process Analytics and Control Technology, Manchester, 28–30 April 2010
69. Scott, G.D., Kilgour, D.M.: The density of random close packing of spheres. J. Phys. D (Brit. J. Appl. Phys.) **2,** 863–866 (1969)
70. Seville, J.P.K., Tüzün, U., Clift, R.: Processing of Particulate Solids. Chapman and Hall, London (1997)
71. Sherman, P.: The viscosity of emulsions. Rheol. Acta **2**, 74–82 (1962)
72. Sherman, P.: Industrial Rheology. Academic, London (1970)
73. Sherman, P. (ed.): Food Texture and Rheology. Academic, New York (1979)
74. Sing, K.S.W., Everett, D.H., Haul, R.A.W., Moscou, L., Pierotti, R.A., Rouquérol, J., Siemieniewska, T.: Pure Appl. Chem **57,** 603–619 (1985) (© 1985 IUPAC)
75. Smith, P.A., Haber, R.A., Am, J.: The effect of particle packing in the filtration and rheology behavior of extended size distribution alumina suspensions. Ceram Soc. **78**, 1737–1744 (1995)
76. Strivens, T.A.: Introduction to rheology (Ch. 14). In: Lambourne, R., Strivens, T.A. (eds.) Paint and Surface Coatings, 2nd edn. Woodhead Publ, New York (1999)
77. Suzuki, M., Sato, H., Hasegawa, M., Hirota, M.: Effect of size distribution on tapping properties of fine powder. Powd. Technol. **118**, 53–57 (2001)
78. Szczesniak, A.S.: Texture is a sensory property. Food Qual. Pref. **13**, 215–225 (2002)
79. Tadros, T.F.: Colloids in Paints. Colloids and Interface Science Series, vol. 6. Wiley-VCH, Weinheim (2010)
80. Tanner, R.I., Walters, K.: Rheology: An Historical Perspective. Elsevier, New York (1998)
81. Taylor, M.K., Ginsburg, J., Hickley, A.J., Gheyas, F.: Composite method to quantify powder flow as a screening method in early tablet or capsule formulation development. AAPS PharmSciTech **1**(3), E18 (2000). doi:article 18
82. US Pharmacoeia 29-NF24 p.3017 <1174 > Powder Flow. http://www.pharmacopeia.cn/v29240/usp29nf24 s0_c1174.html
83. Vadillo, D.C., Tuladhar, T.R., Mulji, A.C., Mackley, M.R.: The rheological characterization of linear viscoelasticity for ink jet fluids using piezo axial vibrator and torsion resonator rheometers. J. Rheol. **54**, 781–795 (2010)
84. Valverde Millán, J.M.: Fluidization of Fine Powders. Particle Technology Series, vol. 18. Springer, Dordrecht (2013)
85. Wagner, N.J., Brady, J.F.: Shear thickening in colloidal dispersions. Phys. Today 27–32, (2009)

86. Weber, H.W.: Lichtstreuung and Teilchengröszenverteilung Kugelförmiger Teilchen. Kolloid Zeitschrift u. Zeitschift f. Polym. **188**, 40–44 (1962)
87. Yu, A.B.., Bridgewater, J., Burbidge, A.: On the modeling of the packing of fine particles. Powd. Technol. **92**, 185–194 (1997)
88. Ziegler, G.R., Mongia, G., Hollender, R.: The role of particle size distribution of suspended solids in defining the sensory properties of milk chocolate. Int. J. Food Prop. $\mathbf{4^2}$, 353–370 (2001)
89. www.giss.nasa.gov/mmischenko/t_matrix.html